Journal of Physics D: Applied Physics

PAPER

Enhancing silica surface deprotonation by using magnetic nanoparticles as heating agents

To cite this article: W Wolak *et al* 2019 *J. Phys. D: Appl. Phys.* **52** 465001

IOP Publishing Journal of Physics D: Applied Physics
J. Phys. D: Appl. Phys. **52** (2019) 465001 (10pp) https://doi.org/10.1088/1361-6463/ab39ff

Enhancing silica surface deprotonation by using magnetic nanoparticles as heating agents

W Wolak[1], A B Kolomeisky[2], M R Dudek[1], M Marć[1] and L Najder-Kozdrowska[1]

[1] Institute of Physics, University of Zielona Góra, ul. Szafrana 4a, 65-069 Zielona Góra, Poland
[2] Center for Theoretical Biological Physics, Rice University 6100 Main Street Houston, TX 77005-1892, United States of America

E-mail: M.Dudek@if.uz.zgora.pl

Received 27 March 2019, revised 24 July 2019
Accepted for publication 9 August 2019
Published 2 September 2019

Abstract

In this work, we investigate the possibility of using magnetic nanoparticles embedded into the silica to locally heat up the silica-water interface where the increase in temperature of nanoparticles is induced by an external radio-frequency magnetic field. Through the use of the theoretical model, it is shown that such the process leads to an increase in the total negative charge of the silica surface due to the deprotonation of silanol groups. It is also shown that the efficiency of such an electric charging process depends on the size of nanoparticles. Moreover, the optimal size of nanoparticles allowing for a maximum charging efficiency is determined. This observation may prove to be very important from the point of view of potential applications as it may allow to fine-tune chemical reactions on the silica surface. Some aspects of this work related to the magnetically heated nanoparticles were verified by the experiment.

Keywords: magnetic nanoparticles, magnetic heating, silica, deprotonation

(Some figures may appear in colour only in the online journal)

1. Introduction

Recent years show a rapidly growing interest of the scientific community in the research related to the use of silica-based materials in medical and biotechnology-oriented applications, e.g. bioimaging [1], magnetic resonance imaging (MRI) [2, 3], protein adsorption [4, 5], drug delivery/release systems [6, 7], bone tissue regeneration [8], hyperthermia [9–11], cell separation [12, 13], catalysis and environmental remediation [14]. The reason for such a large number of studies is the fact that silica is non-toxic and biocompatible which means that it can be conveniently used in order to create new composite materials such as the silica combined with magnetic nanoparticles. In this study, we focus on the particular property of silica surface associated with the fact that the silica-water interface can become electrically charged due to the process of dissociation of terminal silanol groups [1, 15–22]:

$$\mathrm{SiOH} \rightarrow \mathrm{SiO^-} + \mathrm{H^+}. \quad (1)$$

The charge acquired by silica depends on the silanols density, the value of pK of the silanol groups and the pH of the solution contacting the silica [15]. The optical method measurements based on surface second harmonic generation spectroscopy experiment (SHG) indicate the presence of two types of silanol groups on the silica surface where 19% of silanols have a pK of 4.5 and 81% of silanols have a pK of 8.5 [15, 16]. There is still a lot of discussion about the differentiation of silica surface areas due to the value of pK. Analysis of silica surface acidity using the titration method [23] is an important reference point in this discussion. The recent experimental SHG results published by Darlington and Gibbs–Davis [21] suggest the existence of as many as three different surface acidities with pK values of approximately 3.8, 5.2, and 9 but these acidities depend on the initial titration value of pH. Pfeiffer–Laplaud *et al* [20] performed structural studies which are based on *ab initio* molecular dynamics method and they supported the existence of the bimodal character of the amorphous silica surface acidity. Very important for the undergoing

discussion on the silica surface charge is also the paper by Sen and M Barisik [24] which indicates the specificity of mesoporous silica in which case both internal pore surface and external pore surface charge should be considered.

The elaboration of the methods of controlling the electrical charging of the silica surface becomes a new challenge. The use of the single-domain Fe_3O_4 magnetic nanoparticles heated by a radio-frequency magnetic field to influence deprotonation processes which are suggested in this study could be one of such challenges. The small size of such nanoparticles (<15 nm) and high electrical resistivity cause that the heat generated from eddy currents is negligible [25] (see also section 2.1). This is one of the reasons for biomedical applications of the ferrofluids based on the Fe_3O_4 magnetic nanoparticles [26]. The wide discussion on using the magnetocaloric effect of magnetic nanoparticles to medical applications can be found in the paper by Tishin and Spichkin [27]. An interesting status review on using magnetic hyperthermia with magnetic nanoparticles can be found in the recent publication by Salunkhe, Khot and Pawar [28]. In this work, we construct a theoretical model for silica-water interface with magnetic nanoparticles Fe_3O_4 as heating agents. The results related to magnetic heating were supported experimentally.

2. Experimental

2.1. Magnetic nanoparticles synthesis

Magnetic nanoparticles Fe_3O_4 were synthesized through the use of the Massart co-precipitation method [29]. Such synthesis was conducted using glass flask filled with 250 ml of 1.5 M NH_4OH and equipped with a mechanical stirrer. In addition to that, the ammonium base was deoxygenated by nitrogen gas for 30 min. Then, the mechanical stirrer was set to 1.2 krpm and the ultrasonic cleaner was turned on. As a precursor of magnetite nanoparticles, 5.2 g $FeCl_3 \times 6H_2O$ and 2 g $FeCl_2 \times 4H_2O$ diluted in 2 M HCl were used. Subsequently, the solution of the iron chlorides was added dropwise to the flask with ammonium base. As a result, the black suspension was observed. It should be also noted that the product of the synthesis, i.e. magnetic nanoparticles, was separated with a magnet and washed with distilled water with this procedure being repeated five times. Finally, magnetite nanoparticles were dried in 50 °C.

2.2. Preparing silica matrix with magnetic nanoparticles

Magnetic nanoparticles and mesoporous silica (Mesoporous Silica Spheres, Sigma Aldrich) were dispersed separately in a 4 M sodium base water solution and sonicated for 30 min. Diluted silica was added to Fe_3O_4 nanoparticles suspension, obtaining mass ratio of 1:8. After the subsequent 15 min sonication process, the pH of the solution was adjusted to 7 by adding hydrochloric acid. Obtained suspension was washed five times with distilled water. At this point, it should be emphasised that the solution described above was used in the magnetic heating experiments, atomic force microscopy (AFM) measurements and transmission electron microscopy (TEM) measurements that were conducted in this work.

In the magnetic heating experiments, the volume ratio of magnetic nanoparticles and water was equal to $\Phi \sim 0.002$ (5 mg of bare nanoparticles, 0.5 ml of water). In the case of AFM and TEM analyses the prepared suspension was diluted and a drop of the suspension was placed on the respective substrate, where it dried to form of a thin film.

2.3. Measurement characterization

Samples of the silica film filled with magnetic nanoparticles were investigated through the use of the AFM (Nanosurf FlexAFM C3000) and TEM (FEI Tecnai G2 20 X-Twin).

The size of nanoparticles that were synthesised in the experiment was measured using AFM in the case when nanoparticles were distributed uniformly on a fresh mica surface with the area of 20 μm × 20 μm.

In addition to the aforementioned analysis of considered samples, ferromagnetic resonance (FMR) measurements were also conducted. In this case, the resulting FMR spectra were obtained using X-band ($f \sim 9.4$ GHz) EPR spectrometer of the SE/X-2013 type ('RADIOPAN', Poznań, Poland), operating in high-frequency (100 kHz) modulation mode of magnetic field at room temperature.

The final type of measurements corresponded to magnetic heating experiments that were performed with the help of a device for magnetic hyperthermia constructed by us. This device uses the radio-frequency magnetic field generator which is based on a coil made from copper tube which has six turns. The water cooling system is applied where water flows through the coil interior. The radio-frequency magnetic field parameters which were used in the experiment are the following: $f = 100$ kHz, magnetic field amplitude $\mu_0 H_0 = 20$ mT.

3. Experimental results

The experimental part of the research concerns the measurement of the silica-water interface temperature in the case when the silica contains magnetic nanoparticles heated by an external radio-frequency magnetic field. The method used in this work is the placement of previously prepared magnetic nanoparticles in dissolved mesoporous silica and then crystallizing such a material. In order to visualise samples analysed in this work, we used different microscopy-based techniques, i.e. AFM and TEM. The obtained results are summarised in figure 1. In particular, in figure 1(a) the topology of the silica film surface is shown. The presence of magnetic nanoparticles in silica is shown in TEM image (figure 1(b)). The magnetic nanoparticles diameter distribution which was used in all experiments in this work is shown in (figure 1(d)).

Figure 2 shows the results of magnetic heating of two samples of magnetic liquids by the external radio-frequency magnetic field and the results of the ferromagnetic resonance (FMR) spectroscopy for the magnetic material used in both samples. It can be seen in figure 2(a) that the initial rate of

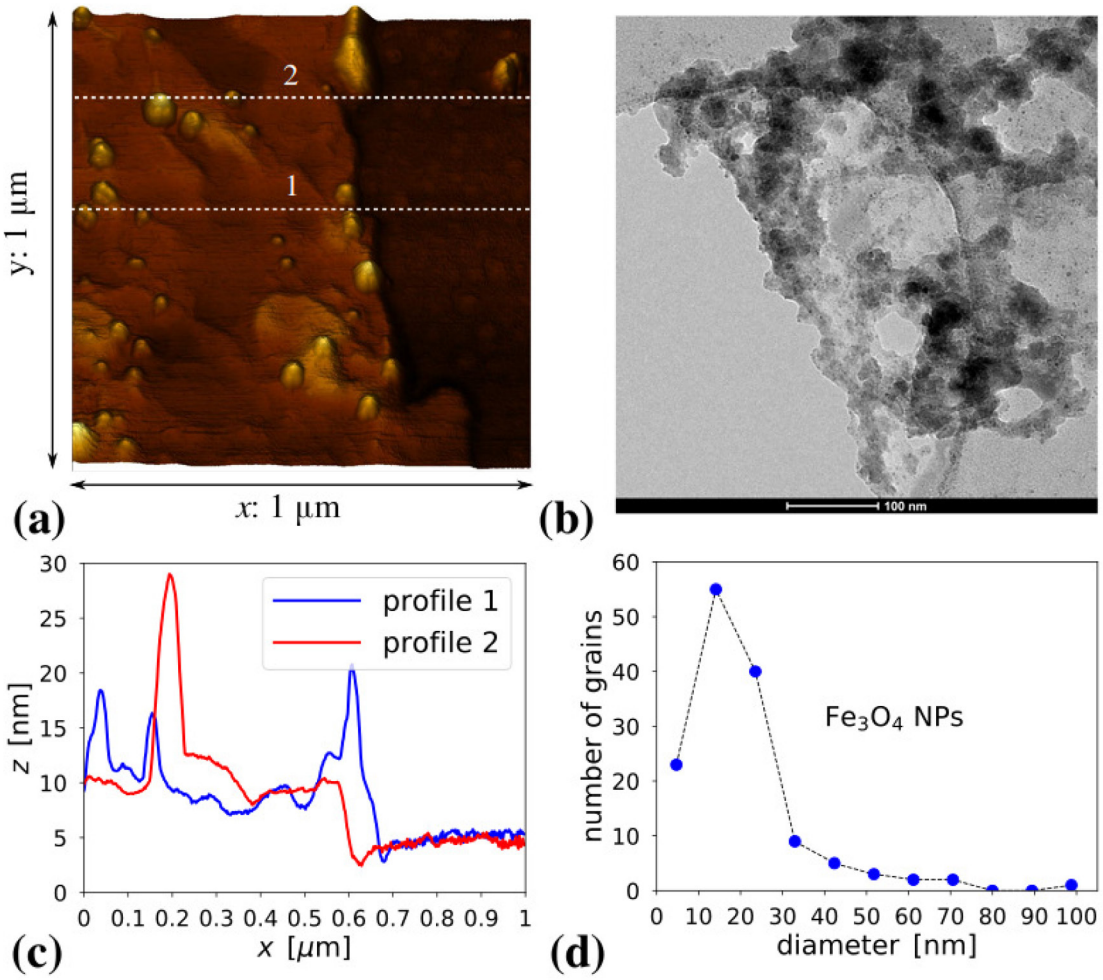

Figure 1. Silica film with magnetic naoparticles: (a) AFM image, (b) TEM image. (c) The height of the sample in the direction corresponding to two crossections denoted as profile 1 and profile 2 with those profiles being also marked by means of dashed white lines in (a) and (d) The size distribution of magnetic nanoparticles obtained by means of AFM measurements from the area of 20 μm $\times$ 20 μm.

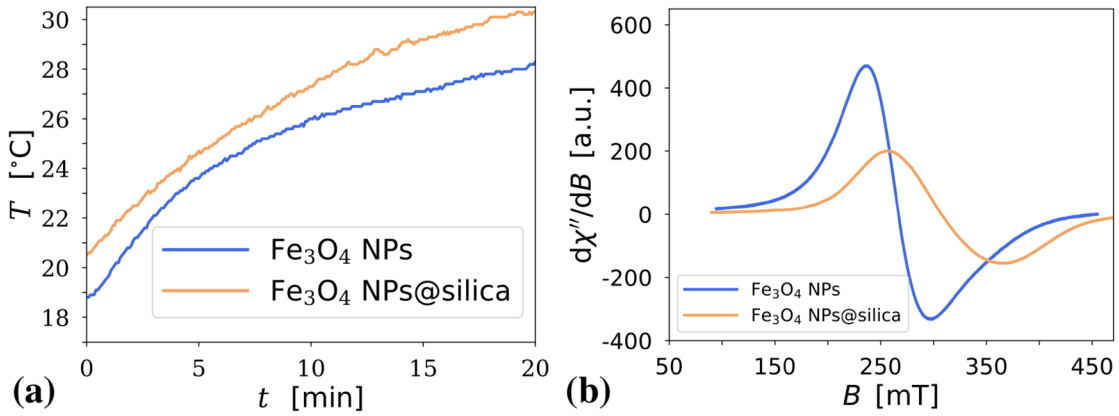

Figure 2. (a) Temperature increase measured in the water suspension of magnetic Fe_3O_4 nanoparticles and in water with the pieces of crystallized silica filled with the Fe_3O_4 nanoparticles. In both cases the samples are exposed to the external radio-frequency magnetic field ($f = 100$ kHz, $\mu_0 H_0 = 20$ mT) by 20 min. The volume of water in the suspensions was 0.5 ml and the volume fraction of the nanoparticles $\Phi \sim 0.002$. The initial temperature: $T_{\text{init}} = 18.8$°C (bare nanoparticles) and $T_{\text{init}} = 20.5$ °C (silica with nanoparticles). (b) Dependence of the absorption line derivatives, $d\chi''/dB$ on the value of the *dc* magnetic field B for the materials used in (a).

the temperature increase $\Delta T/\Delta t$ is lower for the sample with crystallized silica containing magnetic nanoparticles than for the sample with bare nanoparticles. The magnetic properties of the material of both samples were examined by means of the FMR spectroscopy and the results are shown in figure 2(b). The plots in this figure represent the dependence of the absorption line derivatives, $d\chi''/dB$ on the value of the *dc* magnetic field B, where χ'' denotes the imaginary part of the magnetic complex susceptibility. The shift of the resonance field towards higher magnetic field B can be observed compared to the case of using bare nanoparticles. It results from the fact that the axes of magnetic anisotropy of magnetic nanoparticles that are frozen in silica are distributed in different directions. If the axis of the magnetic anisotropy is not parallel to the direction of B then the resonance field becomes shifted to higher values of B [30]. This result justifies the lower value of the initial rate of the temperature increase $\Delta T/\Delta t$ in the case of silica with magnetic nanoparticles. The broadening of the spectral line suggests the presence of small agglomerates of the magnetic nanoparticles. This is consistent with TEM image in figure 1.

4. Model of electric charging the silica-water interface by magnetic heating

In order to analyze the influence of heating the silica-water interface by magnetic nanoparticles on the electric charging the silica surface, we consider a model that is based on the work by Rosensweig [25] where the heating of magnetic fluids with an alternating magnetic field was taken into account. More specifically, in this work, we consider an assembly of separated magnetic single-domain nanoparticles placed in silica that is in a water solution and nanoparticles are exposed to the external radio-frequency magnetic field. The example of the real silica film filled with magnetic nanoparticles is shown in figure 1. It is assumed that the silica surface becomes negatively charged due to the presence of deprotonated silanol groups [17, 23]. In this study, the value of the charge is increased by the localized heating of the silica-water interface by magnetic nanoparticles. This charge is calculated with the help of equations that were derived for deprotonation reactions. It is also worth to emphasize the fact that the considered model is structural. In this case, it means that it consists of the part characterizing the way the temperature increase of the silica-water interface by the heated magnetic nanoparticles is calculated (section 2.1), the part describing the way the deprotonation processes depend on temperature and the value of pH (section 4.2), and the part in which the temperature increase caused by localized magnetic heating is used to describe the electrical charging the silica-water interface (section 4.3).

4.1. Magnetic heating

Theoretical results on magnetic heating of magnetic nanoparticles in a magnetic liquid, which were published by Rosensweig [25], can be easily adapted to magnetic nanoparticles in the silica-water interface where nanoparticles are embedded in silica. An example of such material is shown in figure 1. Also other methods for placing magnetic nanoparticles in silica are possible. If silica has a well-developed porous structure, it can be filled with nanoparticles by a diffusion method [31] or it is possible to synthesise magnetic nanoparticles directly in the pores of the silica [32, 33].

In the theoretical model which is introduced in this study magnetic nanoparticles are placed into silica which is contacting a water solution with a given value of pH. The magnetic nanoparticles are exposed to the external alternating magnetic field $H(t) = H_0\cos(\omega t)$ where $\omega = 2\pi f$ represents angular frequency of the field, $f = 100\,\text{kHz}$, and the field strength $\mu_0 H_0 = 20$ mT, where $\mu_0 = 4\pi \times 10^{-7}$ Tm/A is the magnetic permeability of vacuum. The electromagnetic wave power absorbed by the nanoparticles is proportional to the rate of the temperature increase $\Delta T/\Delta t$, where Δt is the duration of heating. This value, normalized by mass m_{NP} of magnetic nanoparticles, is expressed in terms of the specific absorption rate (SAR) which in units of W kg^{-1} takes the following form:

$$\text{SAR} = C\frac{\Delta T}{\Delta t}, \tag{2}$$

where C is the mass weighted specific heat capacity [34]. In the case of three components, magnetic nanoparticles, silica and water, it reads as:

$$C = \frac{C_w m_w + C_{\text{NP}} m_{\text{NP}} + C_s m_s}{m_{\text{NP}}}, \tag{3}$$

where m_w represents mass of water, m_{NP} is mass of nanoparticles, m_s represents mass of silica, C_{w} is specific heat capacity of water (4185 J kg^{-1} K^{-1}), C_{NP} is the specific heat capacity of magnetic nanoparticles (670 J kg^{-1} K^{-1} for Fe_3O_4 magnetic nanoparticles) and C_s denotes the specific heat capacity of silica (730 J kg^{-1} K^{-1}).

The SAR coefficient in equation (2) is related to the volumetric heating power (in units of W m^{-3}):

$$P = \text{SAR}\frac{m_{\text{NP}}}{V}, \tag{4}$$

which in the case of small magnetic nanoparticles can be expressed exactly as in the Rosensweig's model [25]:

$$P = \frac{1}{2}\mu_0\chi''\omega H_0^2, \tag{5}$$

where χ'' denotes the imaginary part of the magnetic complex susceptibility (equation (9b) in [25]). Then the temperature rise ΔT can be calculated with the help of equations (2), (4) and (5) and it takes the following simple form:

$$\Delta T = \frac{PV}{m_{\text{NP}}C}\Delta t. \tag{6}$$

It is worth to note that the power dissipation (P_e) due to eddy currents in the small single-domain magnetic nanoparticles Fe_3O_4 is smaller by a few orders of magnitude compared to P. This can be shown if we were to assume the following parameters: spherical nanoparticles with the radius of $R_g = 7\,\text{nm}$, magnetic field amplitude $B_0 = 20$ mT, $f = 100\,\text{kHz}$, the electrical conductivity $\sigma = 10^4$ S m^{-1}. In such the case, the

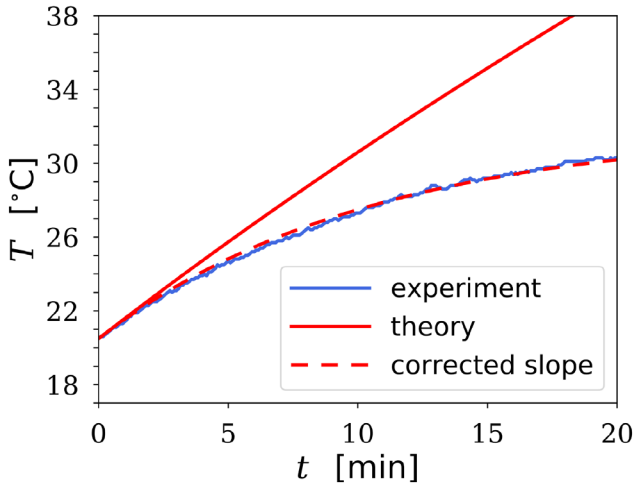

Figure 3. Dependence of temperature T on time t during heating the monodispersion of magnetic nanoparticles with radius $R_g = 6.8$ nm. The result of the corrected slope method was compared with the experimental curve (MNP@silica) in figure 2. The parameters in the theoretical model were taken as in figure 2. The magnetic anisotropy K_a is chosen to be equal to 13.5×10^3 J m^{-3}.

calculated ratio $P_e/P \approx 10^{-8}$ ($P \approx 10^5$ W m^{-3}). This value can be also compared with the heating due to eddy currents in an aqueous solution. In the case of distilled water in a cylinder with radius $r = 0.5$ cm (radius of the eppendorf tube) and $\sigma = 10^{-4}$ S m^{-1} the calculated $P_e/P \approx 4.7 \times 10^{-7}$. In the case of a 10 % NaOH solution ($\sigma = 35.5$ S m^{-1}) the calculated P_e/P would increase to the value of 0.167. It should be noted that silica itself is a source of hydronium ions due to deprotonation processes that can make a significant contribution to the appearance of eddy currents in a water solution in the case of a silica material which has a large surface area to mass ratio. However, it is not the case of the considered model. It should be also noted that expressions for P_e can be found in [35–37].

In the model under consideration, magnetic nanoparticles are immobilized in the silica and the Néel relaxation time of the magnetization becomes dominant in the magnetic relaxation process. In the implementation of numerical issues of magnetic heating, the time unit $\Delta t = 0.01$ was selected and for any time t temperature was calculated as follows: $T(t) = T(t - \Delta t) + \Delta T(t)$, where $\Delta T(t)$ is defined in equation (6). The example of the plot of the calculated temperature increase according to equation (6) is shown in figure 3 (continuous line in red color). However, for magnetic hyperthermia devices, some correction should be made due to the heat energy loss to the environment when the temperature of the sample is higher than that of the temperature T_{init} of the surrounding. A detailed description of the method of including such an adjustment can be found in the recent paper by Wildeboer, Southern and Pankhurst [38]. In their corrected slope method the power P is corrected for any linear losses at temperature T, i.e. $P = C(dT/dt) + L(T - T_{\text{init}})$ where L is a constant. In figure 3, the value of L was optimized in a way that the increase in ΔT is approximately the same as in the experiment. At this point, it should be emphasized that the effect of heating the silica-water interface by nanoparticles placed in silica has a local character. This property may have potential applications, e.g. in conditions where it is necessary to change the value of pH of the silica-water interface locally by increasing the temperature. The analogous concept for local hyperthermia applied to cancerous tumor treatment is widely discussed in recent medical applications [2, 3]. The particular example of the localized heating up by magnetic nanoparticles in the external radio-frequency magnetic field, as shown in the other work by some of the authors [39], might be the use of hyperthermia effect of magnetic nanoparticles Fe_3O_4 to tune the antibody-antigen binding strength. Another example is the pH control of the oriented aggregation which becomes a new challenge for crystallography [40]. Silica is soluble in water and its solubility increases rapidly above pH 8. Its solubility also depends strongly on the temperature [23]. This means that even the local effect of supplying heat to the silica-water interface by magnetic nanoparticles exposed to the external radio-frequency magnetic field can lead to local overheating of silica and its rapid dissolution in aqueous solution. Our estimates show that the temperature increase in the vicinity of a single magnetic nanoparticle of 7 nm placed in water, say at distance of 400 nm from the nanoparticle, is around 1 μ°C after 1μs exposure to the external magnetic field ($f = 100$ kHz, $\mu_0 H_0 = 20$ mT), i.e. $\Delta T/\Delta t \approx 1$ °C s^{-1}.

4.2. Efect of temperature on silica surface charge

In this subsection, we describe the consequences of temperature increase on deprotonation of the silica surface. As a consequence, silica acquires a negative electrostatic charge, the amount of which depends on the value of pH of the aqueous solution in which the silica is placed. The same mechanisms are present if we use magnetic nanoparticles as heating agents with the difference that they are local.

In our model, we assume that the negative charge acquired by silica surface results from the dissociation of the silanol groups Q^3 (≡SiOH) and Q^2 (=Si(OH)$_2$). The chemical reactions representing the dissociation of the isolated groups in Q^3 sites and the geminal groups in Q^2 sites are well known in literature [17, 19, 41, 42]. Experimental data show that in the temperature range 25–190°C all types of silanol groups are present on the silica surface [17] and only further increase in temperature may lead to their degradation. The magnetic nanoparticles which in this study are used in the model of charging silica-water interface represent very weak heat sources and they are not able to degradate silanol groups. Therefore, it has been assumed that the surface fractions $c_1 = 0.19$ of the more acidic Q^3 sites and $c_2 = 0.81$ of the less acidic Q^2 sites are temperature independent. It has been also assumed that the silica surface areas can undergo only the following two deprotonation reactions:

$$\frac{[\mathrm{H^+}]\,[\mathrm{SiO^-}]_1}{[\mathrm{SiOH}]_1} = 10^{-\mathrm{pK_1}}, \tag{7}$$

$$\frac{[\mathrm{H^+}]\,[\mathrm{SiO^-}]_2}{[\mathrm{SiOH}]_2} = 10^{-\mathrm{pK_2}}, \tag{8}$$

representing the more acidic and the less acidic area which are denoted by indices 1 and 2, respectively, and $[\mathrm{H^+}]$ represents the molar concentration of protons. In the model, these two regions of silica surface are separated and it is assumed that the deprotonation processes in them are independent of each other. The values of pK are given experimentally, $\mathrm{pK_1} = 4.5$ and $\mathrm{pK_2} = 8.5$ at temperature 25 °C [15, 16]. It should be emphasized that using only two constants to describe the deprotonation equilibria is a big approximation. They can be considered only as efficient constants. A detailed discussion on the protonation/deprotonation equilibria can be found [23]. In the following, these values of pK are denoted by $\mathrm{pK_1^0}$ and $\mathrm{pK_2^0}$, respectively, and T_0 denotes the corresponding temperature expressed in absolute units (K). An additional assumption in the chemical equilibrium model under consideration is not to take the phenomenon of water autodissociation into account.

Note that in the nonresonant SHG titration experiments some amount of salt is added which may influence the measured value of pK [21]. The current state of knowledge regarding acid-base behavior at the silica-water interface is shortly outlined in Introduction. In this work, we do not discuss the problem of salt addition and its consequences on the acid-base equilibrium. The effect of heated up magnetic nanoparticles on the acid-base equilibrium is discussed instead.

In the model under consideration, the dependence of pK on temperature T is calculated with the help of the integrated form of the van't Hoff equations:

$$\mathrm{pK_1} = \mathrm{pK_0^1} - \frac{\Delta H_0^1}{2.3026R}\left(\frac{1}{T_0} - \frac{1}{T}\right), \tag{9}$$

$$\mathrm{pK_2} = \mathrm{pK_0^2} - \frac{\Delta H_0^2}{2.3026R}\left(\frac{1}{T_0} - \frac{1}{T}\right), \tag{10}$$

where ΔH_0^1 and ΔH_0^2 represent deprotonation energy, 650 kJ $\mathrm{mol^{-1}}$ and 600 kJ $\mathrm{mol^{-1}}$, respectively [20, 43].

In this study, the relative area fractions of the hydroxyl groups SiOH belonging to the silica surface with different acidity are denoted by $f_1 = c_1/(c_1 + 2c_2)$ for the isolated SiOH and $f_2 = 2c_2/(c_1 + 2c_2)$ for the geminal groups. Then, the molar ratio $[\mathrm{SiO^-}]\,/\,[\mathrm{SiOH}]$ in equations (7) and (8) can be expressed by its area counterpart as follows:

$$\frac{[\mathrm{SiO^-}]_1}{[\mathrm{SiOH}]_1} = \frac{x_1}{f_1 - x_1}, \tag{11}$$

$$\frac{[\mathrm{SiO^-}]_2}{[\mathrm{SiOH}]_2} = \frac{x_2}{f_2 - x_2} \tag{12}$$

where x_1 and x_2 represent relative fractions of the deprotonated hydroxyl groups. In the model, the molar concentration $[H^+]$ in equations (7) and (8) depends on surface charge σ of the dissociated silanol groups $\mathrm{Q^2}$ and $\mathrm{Q^3}$ through the electrostatic potential ψ:

$$[H^+] = 10^{-\mathrm{pH}} \mathrm{e}^{-\frac{F}{RT}\psi(x_1,x_2)}, \tag{13}$$

where the value of pH is representing the bulk pH of the water solution, $F = 9.648\,53 \times 10^4$ C $\mathrm{mol^{-1}}$ is Faraday constant, $\mathrm{R} = 8.314$ J $\mathrm{mol^{-1}\ K^{-1}}$ is gas constant, $\psi(x_1, x_2)$ is the electrostatic potential generated by the fractions $x_1 \in [0, f_1]$ and $x_2 \in [0, f_2]$ of the negative electrostatic charge. If Γ denotes the total surface concentration of hydroxyl groups, the total negative surface charge acquired by silica surface reads as the following:

$$\sigma = -\frac{F}{N_A}(x_1 + x_2)\Gamma. \tag{14}$$

The electrostatic potential $\Psi(x_1, x_2)$ can be calculated with the help of the Gouy–Chapman theory by solving Grahame equation [44]. In the linear approximation, it reads as

$$\psi = \frac{\sigma \lambda_D}{\varepsilon_0 \varepsilon}, \tag{15}$$

where λ_D denotes Debye length

$$\lambda_D = \sqrt{\frac{\varepsilon_0 \varepsilon k_B T}{2N_A z^2 e^2 \rho}}, \tag{16}$$

and $\rho = \rho_+ = \rho_-$ is the ion concentration in mol $\mathrm{m^{-3}}$, the ion valence $z = z_+ = \mid z_- \mid = 1$ and $q = \mid z \mid e$, where e is the electronic charge, ε_0 is the permittivity of the free space, ε is dielectric constant of water (in this study we use temperature dependence as in [45]). Finally, after inserting equations equations (13)–(16) into equations (7) and (8) we obtain the following consistent set of two equations describing acid-base equilibrium for deprotonation process of $\mathrm{Q^3}$ and $\mathrm{Q^2}$ sites:

$$\mathrm{pH}_s = \mathrm{pK_1} + \log_{10}\left(\frac{x_1}{f_1 - x_1}\right), \tag{17}$$

$$\mathrm{pH}_s = \mathrm{pK_2} + \log_{10}\left(\frac{x_2}{f_2 - x_2}\right), \tag{18}$$

where pH_s denotes the value of pH at silica-water interface which is related to the value of pH by the following expression,

$$\mathrm{pH}_s = \mathrm{pH} - (x_1 + x_2)\,\frac{F^2 \lambda_D\,\Gamma}{2.3026RTN_A\varepsilon_0\varepsilon}, \tag{19}$$

with $\lambda_D = \lambda_D(T, \rho)$ (equation (16)) at a given value of pH.

Note that for a given value of pH_s the equations (17) and (18) can be solved with respect to x_1 and x_2, i.e.:

$$x_1 = \frac{f_1}{1 + 10^{\mathrm{pK_1} - \mathrm{pH}_s}}, \tag{20}$$

$$x_2 = \frac{f_2}{1 + 10^{\mathrm{pK_2} - \mathrm{pH}_s}}. \tag{21}$$

The plots in figure 4 present the dependence of $x = x_1 + x_2$ representing the negatively charged area of the silica surface on the value of pH_s. The corresponding relationship between the bulk pH and the value of pH_s near the silica surface considering the presence of the electrostatic charge on the surface has been shown in figure 5.

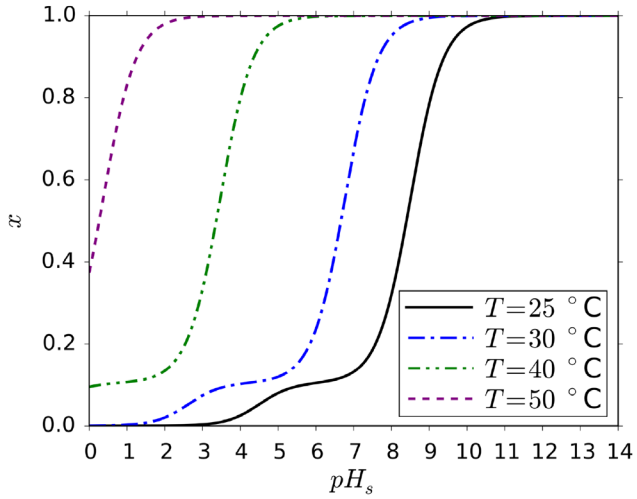

Figure 4. Theoretical model results for the total fraction $x = x_1 + x_2$ of the negative surface charge acquired by silica at a given value of pH_s (equation (19)). The plots represent different temperatures $T = 25, 30, 40, 50$ °C.

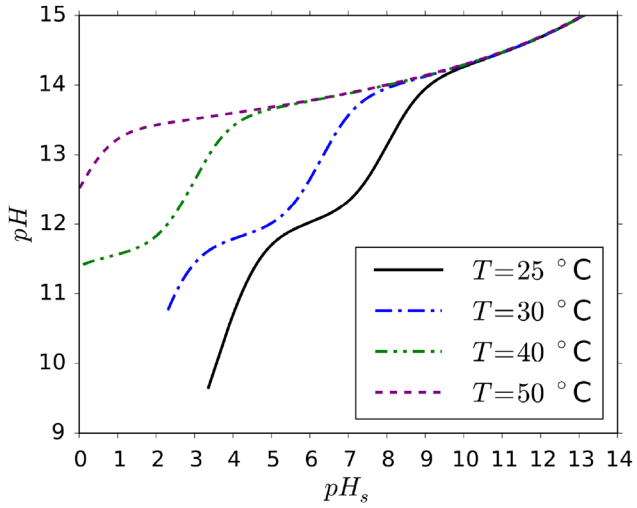

Figure 5. Dependence of the bulk pH on the value of pH_s in the plots presented in figure 4.

4.3. The use of magnetic nanoparticles to charge the silica-water interface

The dependence of the total negative charge acquired by the silica surface on temperature resulting from heating the magnetic nanoparticles can be determined with the help of the equations representing temperature rise ΔT (equation (6)) and chemical equilibrium equations in equations (17) and (18). In the theoretical model under consideration the corrected slope method by Wildeboer, Southern, and Pankhurst [38] was applied to the heating curves. The effect of heating magnetic nanoparticles on the total negative charge fraction x has been shown in figure 6. It should be noted that magnetic nanoparticles represent very small volume fraction ($\Phi \sim 0.2\%$) of the silica-water interface. In the case of a larger fraction, nanoparticles could affect the silanol groups and the value of Γ would be lower. In this work, the value of $\Gamma = 5.0\ \mathrm{nm}^{-2}$ was chosen. The results in figure 6 suggest that the effect of heating up

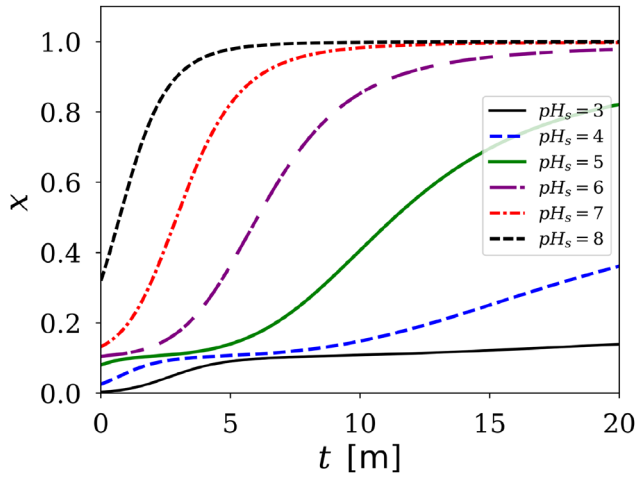

Figure 6. Dependence of the total fraction x of the negative charge at a given value of pH_s on heating time t in the case of a nanoparticle monodispersion ($R_g = 6.8$ nm, $\Phi = 0.002$) incorporated into silica. The plots are made for $\mathrm{pH}_s = 3,4,5,6,7,8$. Initial temperature $T_{\mathrm{init}} = 20$ ° C, $f = 100$ kHz, $\mu_0 H_0 = 20$ mT.

of the magnetic nanoparticles on the increase of the surface negative charge strongly depends on the value of pH of the silica-water interface and duration of the heating. The presence of the low-acidity areas of silica surface is important only at short times of the remote heating of magnetic nanoparticles when the increase of the negative charge is restrained by the persistent step-like structure of the dependence of x on pH_s (see figure 4). However, very important for the potential utilizing of magnetic nanoparticles for electrical charging of the silica-water interface can be figure 7 which shows that the negative charge acquired by the silica surface as a result of magnetic heating depends on the nanoparticle size.

5. Discussion of results

Figure 2(a) shows that even a very small volume fraction $\Phi = 0.002$ of magnetite nanoparticles under radio-frequency magnetic field can increase the temperature of water solution in their vicinity by tens of Celsius degrees in a few minutes. This observation allows the use of magnetic nanoparticles for controlled heating of the silica-water interface. The efficiency of the magnetic heating strongly depends on the quality of the magnetic material. It can be seen in figure 2(b) where the results of the FMR spectroscopy are compared for a powder composed of bare magnetic nanoparticles and a powder being a silica material containing magnetic nanoparticles. The effect of broadening the FMR spectrum lines and the shift of the magnetic resonance field B_r, where χ'' reaches the maximum value, towards the larger values of the *dc* magnetic field B is caused both by the appearance of agglomerates of magnetic particles and the random distribution of the magnetic anisotropy axes of magnetic nanoparticles which are placed in the silica structure. In the FMR experiments, the derivatives of the absorption lines $d\chi''/dB$ are measured instead of χ'' and the value of B_r represents the value of B where $d\chi''/dB = 0$. The weaker magnetic properties of the magnetic nanoparticles

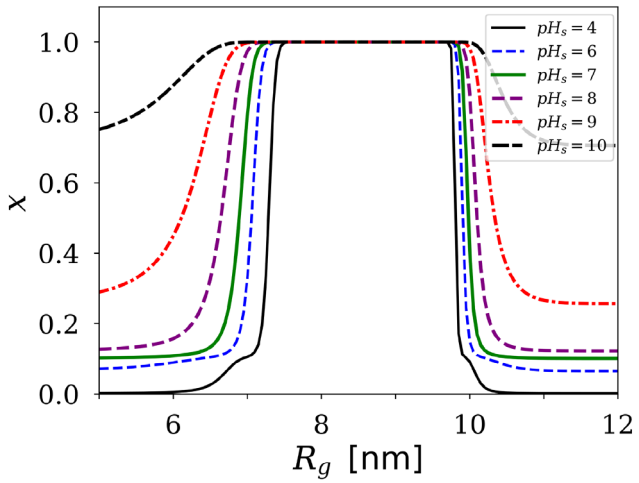

Figure 7. The fraction x of the negative charge acquired by the silica surface as a function of the radius R_g of the nanoparticle monodispersion embedded into silica surface after 5 min of magnetic heating. The plots for different pH_s values are shown. The parameters as in figure 6.

assembly being tested, the greater the value of B_r and the smaller value of χ''. This means that the heating of silica by magnetic nanoparticles in the external radio-frequency magnetic field will significantly depend on the homogeneity of the distribution of the nanoparticles in the silica. Larger agglomerates of the magnetic nanoparticles can lead to local overheating of the silica and consequent its dissolution even near pH 7.

In the experiment from figure 1, magnetic nanoparticles are a polydispersion with the mean value of the nanoparticle size of 12–15 nm. On the other hand, it is well-known that the temperature rise ΔT during magnetic heating strongly depends on the nanoparticle size. Moreover, Rosensweig [25] showed that depending on the type of the magnetic nanoparticles different nanoparticle radius size ranges can have the largest contribution to the heating rate. In the case of Fe_3O_4 magnetic nanoparticles the largest heating rate appears for $R_g \sim 7$ nm. In figure 3, the temperature rise obtained in theoretical model based on Rosensweig theory [25] (equation (6)) has been shown in the case of heating silica-coated nanoparticles with magnetic core radius $R_g \sim 6.8$ nm. For this radius value, the initial heating slope $(\Delta T/\Delta t)$ is as in the experiment in figure 2. Additional adjustment of the theoretical curve (T versus t) using the corrected slope method [38] makes the heating results for the silica-water interface to be close to the experimental ones.

The effect of temperature increase in the silica-water interface (and in related materials) are well known experimentally since years. In particular, in [46] it has been shown that zeta potential of quartz as a function of temperature becomes more negative with increasing temperature. The dependence of the equilibrium fraction $x = x_1 + x_2$ of the deprotonated SiOH groups on the value of the surface pH (denoted by pH_s) has been shown in figure 4. It suggests a strong dependence of the deprotonation process on temperature. The corresponding relationship between the bulk pH of water solution and the value of pH_s at the silica-water interface has been presented in figure 5. It was calculated numerically from equation (19) which is non-linear with respect to pH. Only the solutions which appeared to be numerically stable were plotted. Note that in the model under consideration, the protonation processes have not been included and therefore the acidic values of the bulk pH are not well represented in the model. The stable branches of the dependence of pH on pH_s, which are shown in figure 5, may loss their stability for solutions with different ionic strength.

The dependence of the total negative charge acquired by the silica surface on temperature resulting from heating the magnetic nanoparticles can be determined with the help of the equations representing temperature rise ΔT (equation (6)) and chemical equilibrium equations in equations (17) and (18). In the theoretical model under consideration the corrected slope method by Wildeboer, Southern, and Pankhurst [38] was applied to the heating curves. The effect of heating magnetic nanoparticles on the total negative charge fraction x has been shown in figure 6. It should be noted that magnetic nanoparticles represent very small volume fraction ($\Phi \sim 0.2\%$) of the silica-water interface. In the case of a larger fraction, nanoparticles could affect the silanol groups and the value of Γ would be lower. In this work, the value of $\Gamma = 5.0$ nm^{-2} was chosen. The results in figure 6 suggest that the effect of heating up of the magnetic nanoparticles on the increase of the surface negative charge strongly depends on the value of the surface pH and duration of the heating. The presence of the low-acidity areas of silica surface is important only at short times of the remote heating of magnetic nanoparticles when the increase of the negative charge is restrained by the persistent step-like structure of the dependence of x on pH_s (see figure 4). However, very important for the potential utilizing of magnetic nanoparticles for electrical charging of the silica-water interface can be figure 7 which shows that the negative charge acquired by the silica surface as a result of magnetic heating depends on the nanoparticle size. This result is a direct consequence of the finding by Rosensweig [25] in the field of ferrofluids that the heating rate of the system of magnetic nanoparticles strongly depends on the size of the nanoparticles. In addition, the charging process is efficient only for a narrow range of magnetic nanoparticle radius R_g. The smaller value of pH the stronger limitation for charging the silica surface is by the method of magnetic heating. Some of the parameters determining the magnetic properties of magnetic nanoparticles depend on parameters like magnetic anisotropy constant K_a which can shift the range of the values of R_g where the enhanced charging of the silica surface is observed to the smaller values. This means that using magnetically modified silica material, e.g. in hyperthermia applications requires the high quality single-domain magnetic nanoparticles with the narrow size distribution. This observation may also prove to be important for selective heating up of the silica areas with different acidities. In the case of application of the model to localized hyperthermia therapy a more detailed consideration of the heat flow in tissue is required. One of the possibility is the use of the Pennes bioheat equation, e.g. as in [47].

6. Conclusions

In this work, magnetic iron oxide nanoparticles under the external radio-frequency magnetic field, which were embedded into silica, were used in order to heat up the silica-water interface. The consequence of the increased temperature was an increase in the negative charge on the silica surface due to the dissociation of the silanol groups. The most important result is finding that only nanoparticles with the narrow range of size can achieve the large charging rate of the aforementioned silica-water interface. This work is the first step towards providing a quantitive description of the process corresponding to the possibility of charging the silica-water interface with the help of the magnetic nanoparticles. The presented results can appear to be useful in medical applications and catalysis.

Acknowledgments

We thank H Adamek for measurements on a magnetic hyperthermia device and A Drzewiecki for FMR spectroscopy measurements. W W, M R D, M M and L N-K acknowledge the financial support from the program of the Polish Ministry of Science and Higher Education under the name 'Regional Initiative of Excellence' in 2019–2022, Project No. 003/RID/2018/19, funding amount 11 936 596.10 PLN.

ORCID iDs

A B Kolomeisky https://orcid.org/0000-0001-5677-6690
M R Dudek https://orcid.org/0000-0001-8908-3006

References

[1] Gomes M C, Cunha A, Trindade T and Tome J P C 2016 The role of surface functionalization of silica nanoparticles for bioimaging *J. Innovative Opt. Health Sci.* **9** 1630005
[2] Hurley K R *et al* 2016 Predictable heating and positive MRI contrast from a mesoporous silica-coated iron oxide nanoparticle *Mol. Pharmaceutics* **13** 2172–83
[3] Cantillon-Murphy P, Wald L L, Zahn M and Adalsteinsson E 2010 Proposing magnetic nanoparticle hyperthermia in low-field MRI *Concepts Magn. Reson. Part* A **36** 36
[4] Shir I B, Kababya S and Schmidt A 2014 Molecular details of amorphous silica surfaces determine binding specificity to small amino acids *J. Phys. Chem.* C **118** 7901
[5] Moerz S T and Huber P 2015 pH-Dependent selective protein adsorption into mesoporous silica *J. Phys. Chem.* C **119** 27072–9
[6] Baeza A, Guisasola E, Ruiz-Hernández E and Vallet-Regí M 2012 Magnetically triggered multidrug release by hybrid mesoporous silica nanoparticles *Chem. Mater.* **24** 517–24
[7] Moyano D F and Rotello V M 2011 Nano meets biology: structure and function at the nanoparticle interface *Langmuir* **27** 10376–85
[8] Vallet-Regí M and Balas F 2008 Silica materials for medical applications *Open Biomed. Eng. J.* **2** 1–9
[9] Pankhurst Q A, Connolly J, Jones S K and Dobson J 2003 Applications of magnetic nanoparticle in biomedicine *J. Phys. D: Appl. Phys.* **36** R167–81
[10] Soleymani M and Edrissi M 2015 Heating ability and biocompatibility study of silica-coated magnetic nanoparticles as heating mediators for magnetic hyperthermia and magnetically triggered drug delivery systems *Bull. Mater. Sci.* **38** 1633–8
[11] Dríždal T, Togni P, Víšek L and Vrba J 2010 Comparison of constant and temperature dependent blood perfusion in temperature prediction for superficial hyperthermia *Radioengineering* **19** 281–9
[12] Pertoft H and Laurent T C 1977 Isopycnic separation of cells and cell organelles by centrifugation in modified colloidal silica gradients *Methods of Cell Separation. Biological Separations* ed N Catsimpoolas (Boston, MA: Springer)
[13] Zhao W, Gu J, Zhang L, Chen H and Shi J 2005 Fabrication of uniform magnetic nanocomposite spheres with a magnetic core/mesoporous silica shell structure *J. Am. Chem. Soc.* **127** 8916–7
[14] Sharma V K, Doong R-A, Kim H, Varma R S and Dionysiou D D 2016 *Ferrites and Ferrates: Chemistry and Applications in Sustainable Energy and Environmental Remediation* (*ACS Symp. Series*) (Washington, DC: American Chemical Society)
[15] O'Reilly J P, Butts C P, I'Anson I A and Shaw A M 2005 Interfacial pH at an isolated silica-water surface *J. Am. Chem. Soc.* **127** 1632–3
[16] Ong S, Zhao X and Eisenthal K B 1992 Polarization of water molecules at a charged interface: second harmonic studies of the silica/water interface *Chem. Phys. Lett.* **191** 327
[17] Zhuravlev L T 2000 The surface chemistry of amorphous silica. Zhuravlev model *Colloids Surf.* A **173** 1
[18] Behrens S H and Grier D G 2001 The charge of glass and silica surfaces *J. Chem. Phys.* **115** 6716
[19] Petersen P B and Saykally R J 2006 Comment on Interfacial pH at an isolated silica-water surface *J. Phys. Chem.* B **110** 15037
[20] Pfeiffer-Laplaud M, Costa D, Tielens F, Gaigeot M P and Sulpizi M 2015 Bimodal acidity at the amorphous silica/water interface *J. Phys. Chem.* C **119** 27354
[21] Darlington A M and Gibbs-Davis J M 2015 Bimodal or trimodal? the influence of starting pH on site identity and distribution at the low salt aqueous/silica interface *J. Phys. Chem.* C **119** 16560
[22] Nawrocki J 1997 The silanol group and its role in liquid chromatography *J. Chromatogr.* A **779** 29
[23] Iler K R 1979 *The Chemistry of Silica: Solubility, Polymerization, Colloid and Surface Properties, and Biochemistry* (New York: Wiley)
[24] Sen T and Barisik M 2019 Internal surface electric charge characterization of mesoporous silica *Sci. Rep.* **9** 137
[25] Rosensweig R E 2002 Heating magnetic fluid with alternating magnetic field *J. Magn. Magn. Mater.* **252** 370–4
[26] Ghosh R *et al* 2011 Induction heating studies of Fe3O4 magnetic nanoparticles capped with oleic acid and polyethylene glycol for hyperthermia *J. Mater. Chem.* **21** 13388
[27] Tishin A M and Spichkin Y I 2014 Recent progress in magnetocaloric effect: mechanisms and potential applications *Int. J. Refrig.* **37** 223
[28] Salunkhe A B, Khot V M and Pawar S H 2014 Magnetic hyperthermia with magnetic nanoparticles: a status review *Curr. Top. Med. Chem.* **14** 572
[29] Massart R 1981 Preparation of aqueous magnetic liquids in alkaline and acidic media *IEEE Trans. Magn.* **17** 1247–8
[30] Owens F J 2003 Ferromagnetic resonance of magnetic field oriented Fe3O4 nanoparticles in frozen ferrofluids *J. Phys. Chem. Solids* **64** 2289
[31] Zapotoczny B, Dudek M R, Guskos N, Kozioł J J, Padlyak B V, Kosmider M and Rysiakiewicz-Pasek E 2012 FMR study of the porous silicate glasses with

Fe_3O_4 magnetic nanoparticles fillers *J. Nanomaterials* **2012** 341073

[32] Zapotoczny B, Guskos N, Kozioł J J and Dudek M R 2015 Preparation of the narrow size distribution USPIO in mesoporous silica for magnetic field guided drug delivery and release *J. Magn. Magn. Mater.* **374** 96–102

[33] Jiao F, Jumas J-C, Womes M, Chadwick V, Harrison A and Bruce P G 2006 Synthesis of ordered mesoporous Fe_3O_4 and γ-Fe_2O_3 with crystalline walls using post-template reduction/oxidation *J. Am. Chem. Soc.* **128** 12905

[34] Gonzalez-Fernandez M A, Torres T E, Andrés-Vergés M, Costo R, de la Presa P, Serna C J, Morales M P, Marquina C, Ibarra M R and Goya G F 2009 Magnetic nanoparticles for power absorption: optimizing size, shape and magnetic properties *J. Solid State Chem.* **182** 2779

[35] Jordan A, Wust P, Fählin H, John W, Hinz A and Felix R 1993 Inductive heating of ferrimagnetic particles and magnetic fluids: physical evaluation of their potential for hyperthermia *Int. J. Hyperth.* **9** 51–68

[36] Dutz S and Hergt R 2013 Magnetic nanoparticle heating and heat transfer on a microscale: basic principles, realities and physical limitations of hyperthermia for tumour therapy *Int. J. Hyperth.* **29** 790–800

[37] Sunday K Jo, Hanejko F G and Taheri M L 2017 Magnetic and microstructural properties of Fe_3O4-coated Fe powder soft magnetic composites *J. Magn. Magn. Mater.* **423** 164–70

[38] Wildeboer R R, Southern P and Pankhurst Q A 2014 On the reliable measurement of specific absorption rates and intrinsic loss parameters in magnetic hyperthermia materials *J. Phys. D: Appl. Phys.* **47** 495003

[39] Mleczko J, Defort A, Kozioł J J, Nguyen T T, Mirończyk A, Zapotoczny B, Nowak-Jary J, Gronczewska E, Marć M and Dudek M R 2016 Limitation of tuning the antibody-antigen reaction by changing the value of pH and its consequence for hyperthermia *J. Biochem.* **159** 421

[40] Burrows N D, Hale C R H and Penn R L 2013 Effect of pH on the kinetics of crystal growth by oriented aggregation *Cryst. Growth Des.* **13** 3396

[41] Zhao X, Ong S, Wang H and Eisenthal K B 1993 New method for determination of surface pKa using second harmonic generation *Chem. Phys. Lett* **214** 203

[42] Lowe B M, Skylaris C K and Green N G 2015 Acid-base dissociation mechanisms and energetics at the silica-waterinterface: an activationless process *J. Colloid Interface Sci.* **45** 231

[43] Tielens F, Gervais C, Lambert J F, Mauri F and Costa D 2008 *Ab initio* study of the hydroxylated surface of amorphous silica: a representative model *Chem. Mater.* **20** 3336

[44] Butt H J, Graf K and Kappl M 2003 *Physics and Chemistry of Interfaces* (New York: Wiley)

[45] Malmberg C G and Maryott A A 1956 Dielectric constant of water from 0° to 100 °C *J. Res. Natl Bur. Stand.* **56** 369131

[46] Rammachandran R and Somasundaran P 1986 Effect of temperature on the interfacial properties of silicates *Colloids Surf.* **21** 355

[47] Kuznetsov A V 2006 Optimization problems for bioheat equation *Int. Commun. Heat Mass Transfer* **33** 537